Thermodynamical and microscopic properties of turbulent transport in the edge plasma

2012 J. Phys.: Conf. Ser. 401 012007

(http://iopscience.iop.org/1742-6596/401/1/012007)

Journal of Physics: Conference Series **401** (2012) 012007 doi:10.1088/1742-6596/401/1/012007

Thermodynamical and microscopic properties of turbulent transport in the edge plasma

Ph Ghendrih[1], C Norscini[1], F Hasenbeck[1,2], G Dif-Pradalier[1], J Abiteboul[1], T Cartier-Michaud[1], X Garbet[1], V Grandgirard[1], Y Marandet[3], Y Sarazin[1], P Tamain[1], D Zarzoso[1]

[1]CEA-IRFM, F-13108 Saint-Paul-lez-Durance, France
[2]IEK-4 Plasma Physics, Forschungszentrum Jlich GmbH, Jlich, Germany
[3]PIIM, CNRS/Aix-Marseille Univ., Marseille, France

E-mail: philippe.ghendrih@cea.fr

Abstract. Edge plasma turbulence modelled with 2D interchange is shown to exhibit convective transport at the microscale level. This transport property is related to avalanche like transport in such a flux-driven system. Correlation functions and source modulation are used to analyse the transport properties but do not allow one to recover the Fick law that must characterise the system at large scales. Coarse graining is then introduced to average out the small scales in order to recover the Fick law. One finds that the required space averaging is comparable to the system size while the time averaging is comparable to the confinement time. The system is then reduced to a single reservoir such that transport is characterised by a single scalar, either the diffusion coefficient of the Fick law or a characteristic evolution time constant.

1. Introduction

The widely used diffusion approximation of transport modelling traces back to Einstein's interpretation of the Brownian motion later followed by the Langevin's toy model addressing the same problem [1]. These lead to the picture of a Markov chain of random steps associated to a random time that governs the transport at the microscopic level. An important consequence has been the interpretation it provides for the Fick law of proportionality between the transported flux and the particle gradients, the proportionality coefficient being the diffusion coefficient. However, it must be stressed that the Fick law must be satisfied at the macroscopic level even when the microscopic transport is not associated to diffusion. There appears therefore a scale separation between the microscopic physics that drive the transport and the macroscopic scale where thermodynamics require a Fick law to be satisfied. The key issue is therefore to determine those macroscopic scales such that the system, at these scale, is sufficiently close to thermodynamical equilibrium to recover the proportionality between the flux and the thermodynamical force. We address this problem here in the framework of turbulent plasma in a model where the microscopic transport is governed by turbulence, Section 2, and is found to be predominantly convective, Section 3. A coarse graining process is then introduced to recover the Fick law and to determine the macroscale of the problem, Section 4.

2. Steady state conditions with 2D interchange turbulence in the edge plasma

The present most advanced models of plasma turbulence are addressed in the gyrokinetic framework, hence determining the plasma distribution function f with global full-f and most importantly *flux-driven* codes [2, 3]. It has been reported that flux driven gyrokinetic simulations exhibit avalanche-like transport [4, 5], thus confirming the results obtained with fluid codes [6]. In this paper we use fluid simulations prior to analysing gyrokinetic simulations. The model is the same as in the seminal paper [6]. It is a simple 2-fields and 2D interchange model describing the pressure nT and vorticity W in the plane transverse to the magnetic field. Its structure is identical to that of the Rayleigh-Bénard system that describes convective instabilities. The buoyancy driven transport is the vorticity equation is governed by the magnetic curvature effect in the plasma model while the stream function is replaced by the electric potential. In the plasma model we consider for simplicity a constant temperature $T = T_e$, the electron temperature, so that one actually addresses particle transport in the cold ion limit and not thermal energy as in Rayleigh-Bénard. A key difference between the neutral fluid and the plasma model is the existence, in the latter, of a loss term in the vorticity equation that linearly stabilises the large structures. Consequently, the $E \times B$ convective cells do not reach the size of the system and boundary layer issues are less stringent than in Rayleigh-Bénard experiments and simulations. The a-dimensional equations take the following form:

$$\partial_t n + [\phi, n] - D\Delta n = -\sigma_n(n, \phi)\ n + S \tag{1}$$

$$\partial_t W + [\phi, W] - \nu\Delta W + g\partial_y n = \sigma_\phi(\phi) \tag{2}$$

The vorticity W is directly connected to the electric potential ϕ, normalised to T_e/e, by a Poisson equation $W = \nabla_\perp^2 \phi$. Six control parameters are obtained that govern the drive and loss terms. The linear instability is governed by the existence of the g-term of the order of ρ_s/R, where ρ_s is the hybrid Larmor radius that is introduce to normalise the transverse scales, and R the major radius of the device that drives the magnetic field curvature. The system is driven out of equilibrium by the particle source term S. In the present setting, the source is constant in the y-direction, akin to the poloidal direction, with Gaussian-peaking in the x-direction, akin to the radial direction. The loss term $\sigma_n(n, \phi)\ n$ is characteristic of the SOL region and corresponds to the parallel particle loss term to the wall. The structure of the control parameter $\sigma_n(n, \phi)$, and its possible dependence on ϕ to account for the sheath effects, is of little relevance in the present paper. A key aspect of this term is that this particle loss is distributed in the whole domain, it is therefore a volumetric sink. Indeed, each point in the 2D plane of interest is connected via the third dimension to a limiter surface. The finite confinement time along this direction, and plasma neutralisation at the wall thus governs the particle loss. When steady state conditions are achieved, this volumetric particle loss balances the particle source. Turbulent transport is thus organised from the source region, along the direction of symmetry of the source, the x-direction. The linear interchange instability sets in for negative density gradients, hence in the region localised on the right hand side of the source. Two diffusive transport coefficients are introduced, D and ν. These are normalised to the Bohm value $\rho_s c_s$ (where c_s is the sound velocity) and are small, equal to 10^{-2} in the present work. They are important in damping the small scales that build-up in the turbulent regime.

The last control parameter is the parallel current loss term $\sigma_\phi(\phi)$. Its exact structure, including or not sheath effects, is not crucial here. However, it must be stressed that it takes into account parallel current exchange that can be complex, and will depend on the electric potential, but that does depend explicitly on the vorticity $W = \nabla_\perp^2 \phi$. Consequently, as stated above, it will appear as $-\sigma_\phi/k_\perp^2$ in the calculation of the linear growth rates. Here $k_\perp$ is the wave vector in the plane orthogonal to the direction of the parallel current losses and stems from inverting the vorticity in Fourier space to recover the potential. Conversely, σ_ϕ can depend on

the parallel wave vector $k_\parallel$. The term σ_ϕ thus drives a stabilisation the large mode structures $k_\perp \to 0$. In the present work, it is chosen independent on the density n so that this mechanism is homogeneous throughout the system. Consequences are two fold, first one can consider that it constrains the zonal flows, $k_y = 0$ where y is the poloidal direction. These must then have sufficient radial structure (x-direction) to yield finite values of $k_\perp$ and exhibit weak damping, σ_ϕ being a small parameter. This tends to preserve the shearing properties of the zonal flows but smears out global radial structures of the electric field. Another consequence is that the large scales of the system are stable with respect to turbulence. This favours the existence of macroscales where thermodynamics can apply.

The code solving equations (1, 2) is periodic in both x and y directions. Although the x-periodicity can be considered as unphysical, it allows one to investigate the plasma response in three regions, see figure 1. Due to the symmetry breaking set by the linear criterion for the turbulence onset, most of the simulation domain is governed by turbulent transport, while the region without turbulence, labeled region-III, in a narrow poloidal band that plays a crucial role numerically by preventing cross talk of turbulence in the radial direction, typically this region is characterised by $x \geq 439$ at the minimum of the density profile. Where turbulence governs transport, one labels region-I the region with nearly constant density gradient length $L_n \approx \lambda_n$, and region-II the region where L_n varies radially increasing from $L_n \approx \lambda_n$ to ∞ in the crossover region between the region with turbulent transport and region-III without. A fourth region should be mentioned, that of the particle source, located at $x = 1$ up to $x \approx 16$.

The curvature of the magnetic field and the geometry of the source break the symmetry between the x and y directions. Indeed, the source is constant in the y-direction, so that transport is organised along the x-direction. In this direction, translation invariance is thus broken by the source term. Conversely, the y-direction still exhibits translation invariance that allows one to average in the y-direction to gain in statistics (this is equivalent to a flux surface average). The curvature of the magnetic field drives the instability and leads to the g-term with an explicit dependence on y. In this model, it does not depend on x so that it does not generate extra thermodynamical forces. The average density and particle flux are plotted on figure 1. These are averaged on y and time for the whole simulation duration t_s. It is interesting to note that both density $\langle n \rangle_{y,t_s}$ and radial particle flux $\langle \Gamma_x \rangle_{y,t_s}$ exhibit an exponential fall-off as expected in the SOL plasma. However, it must be stressed that such an exponential fall-off is consistent with both purely diffusive and convective transport and thus cannot be identified as a signature of diffusive transport.

Statistics of these fields, at given x-value, lead to heavy tails Probability Density Functions as shown for Γ_x and $< \Gamma_x >_y$ on figure 2. Remarkable features are attached to these PDF. Let us first consider the PDF of Γ_x, black curve with open o-symbols, attached to the lower scale. First negative values of the particle flux account for a significant part of the data, hence driving particles from the sink towards the source. This result is in fact consistent with the properties of $E \times B$ eddy convection that does not discriminate directions. More unexpected is the fact that the most likely particle flux is negative, one the left hand side of the zero line (vertical dash-dot line). Second, one finds a heavy tail towards the large positive values of the particle flux. Since the small magnitude events are both positive and negative with high but nearly symmetric probability density, they tend to cancel out when addressing the mean value of the radial particle flux. From that point of view, one can state that the effective particle flux (the mean value) is essentially sustained by the heavy tail part of the PDF. This property is specific of flux driven system where the only constraint on the system is to ensure a balance, on average only, between the source and the sink. The heavy tails structures also appear to exhibit avalanche-like

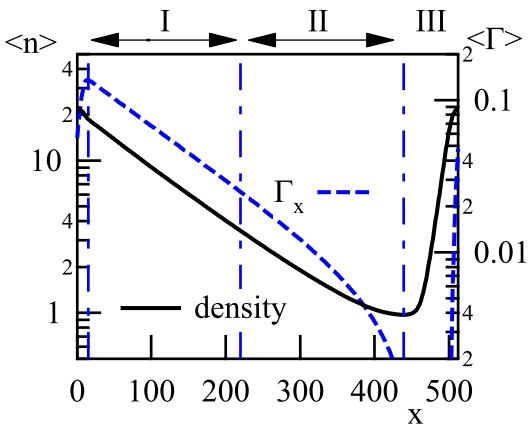

Figure 1. Averaged density and particle flux profiles, regions I, II and III are indicated.

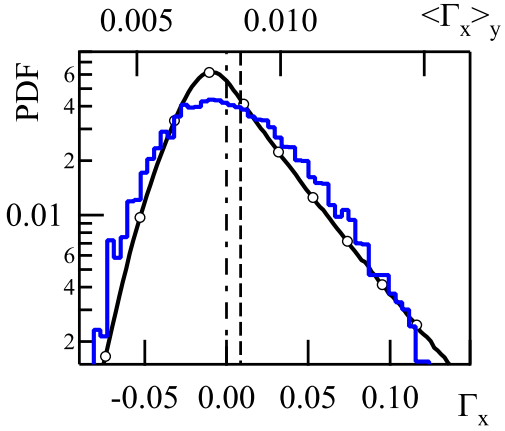

Figure 2. PDF of the particle flux, black curve open o symbols Γ_x lower scale, blue histogram $< \Gamma_x >$ upper scale.

behaviours with 1/f frequency spectra [6]. In the case of SOL plasmas, it can be connected to the so-called blob phenomenology later advocated in ref.([7]). Regarding the negative particle flux events, only an averaging procedure allows one to recover the thermodynamically expected sign of the particle flux. In fact the y-average is found to be sufficient for this process as exemplified by the PDF of $< \Gamma_x >_y$, also on figure 2, blue histogram upper scale. Only positive values are found for $< \Gamma_x >_y$ so that the PDF can be fitted with a lognormal PDF. More importantly is the strong change in the range of the fluctuations, typically a factor 10 between the lower and upper scale. For convenience the two PDF are centred at the same location of their mean value (which is of course identical) as indicated by the vertical dashed line. Despite the sharp drop in the fluctuation level, this PDF still exhibits a heavy tail. Consistently with the discussion of the PDF of Γ_x, one can consider that most of the data contributing to the PDF of $< \Gamma_x >_y$ must therefore stem from avalanche-like events.

The convergence towards a statistical steady state of this turbulence model is slow. To investigate this aspect we analyse the local convergence for each point in y, at the same x position of $\langle \Gamma_x \rangle_t$ when varying the duration t of the averaging process. We can then plot the distance $\left| \langle \Gamma_x \rangle_t - \langle \Gamma_x \rangle_{y,t_s} \right|$, see figure 3. One finds that the convergence takes place according to the scaling law $1/\sqrt{N}$ where N is the number of events. Fitting the data indicates that an event corresponds in fact to a finite duration τ_N, as indicated by the vertical dashed line on figure 3. This duration of a typical event must be compared to the confinement time of the system defined as $\tau_E = 1/\sigma_n$. Indeed, one can readily show that when switching off the source term, the total number of particles in the simulation domain will decay exponentially with e-folding time $\tau_E = 1/\sigma_n$. The simulation evidence thus leads to $\tau_N \approx \tau_E/6$. The events last a significant fraction of the confinement time. To complete the discussion on the characteristic times, another key time must be introduced, namely the turbulence correlation time τ_c. Data from the simulation yields $\tau_c \approx \tau_E/32$, figure 4. The typical event duration is thus in the range of 5 correlation times, a ratio also reported in gyrokinetic flux driven simulations [4]. When compared to the total simulation time $t_s \approx 40\tau_E$, one thus finds that typically 240 events take place. Together with the very irregular decay noticeable on figure 3, this large but not very

large number of events underlines the difficulty in obtaining sufficient statistics to determine with precision the steady state regime.

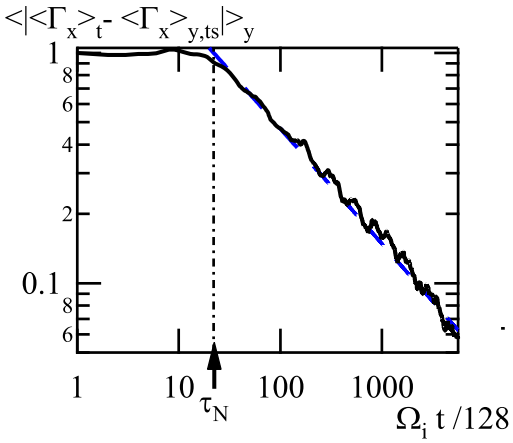

Figure 3. Convergence of the particle flux towards its mean value.

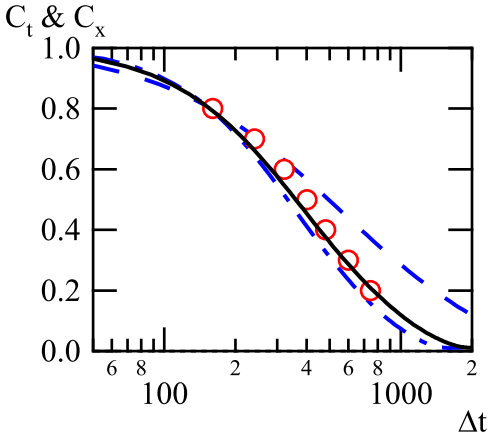

Figure 4. Time, $\mathcal{C}_t$ open circles, and space $\mathcal{C}_x$ correlation functions for $\alpha = 1.1$ plain, $\alpha = 1.5$ dashed and $\alpha = 1.0$ dash-dot lines.

3. The microscopic turbulent transport

The investigation of the microscopic turbulent transport has been undertaken with several approaches. Starting from the description of the transport in the set of equations (1, 2), one finds that in the turbulent regime the transport is governed by $E \times B$ convection. At the microscopic level, the issue is determining the sequence of events that bound this correlated convective motion, thus defining step sizes and step durations for the transport process. The PDF of these step characteristics will then govern the nature of the microscopic transport. In practice this approach is difficult to implement for turbulence since the decorrelation process that bounds the steps is not well defined. A standard alternative is to address the transport of test particles governed by the time dependent $E \times B$ motion. Investigating the time dependence of the mean distance between the test particles and their initial position with the present model in [6] indicates that the test particle transport is close to ballistic. A more demanding analysis is based on tracing the large flux events and determining their dynamics. One then finds that the events first experience an acceleration before propagating with a nearly constant velocity, hence behaving like fronts or avalanches. Since these large events dominate the average flux, it then appears that the microscopic transport is essentially ballistic [8]. A third approach proposed here is based on self similarity of transport such that the appropriate variable is x/t for ballistic transport and x^2/t for diffusive transport. Generalising this similarity constraint to turbulence transport, one expects transport to depend on x^α/t, the exponent α characterising the nature of transport. We then match the self-correlation function in time $\mathcal{C}_t(\Delta t)$ and self-correlation in space along the x-direction $\mathcal{C}_x(\Delta x)$ so that: $\mathcal{C}_t(\Delta t) \approx \mathcal{C}_x(c\ \Delta x^\alpha)$. In log scale for the abscissa, the constant c is determined as an offset while the parameter α governs the slope, figure 4. This procedure yields $\alpha \approx 1.1$ and $c \approx 15$, see figure 4, hence a value close to ballistic $\alpha = 1$ and clearly not diffusive $\alpha = 2$. This result is surprising since in the standard approach *à la mixing length* would stipulate the transport to be diffusive, the diffusion coefficient being $D_c = \lambda_c^2/\tau_c$ where $\lambda_c \approx 24$ is the correlation length. The correlation length and correlation time would then define the elementary event, and assuming a Markov process would govern the diffusive

transport for scales larger than that of the elementary event. Given the values of λ_c and τ_c one then expects a diffusive coefficient $D_c \approx 1.11$ (normalised to the Bohm diffusion), typically 100 times larger than the small scale smoothing diffusion D. However, should one assume that the sign of the step is not random but always positive, the sequence of elementary events will lead to a ballistic transport of magnitude $V_c = \lambda_c \tau_c \approx 0.046$ (normalised to the sound velocity, and therefore effectively a Mach number) not too different from the upper bound value $1/c \approx 0.067$.

The different approaches used in analysing the microscopic transport properties indicate that the microscopic transport is close to ballistic in marked difference with that assumed when considering the Brownian motion.

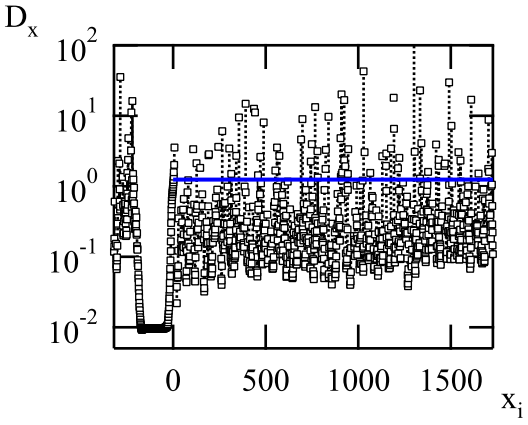

Figure 5. Diffusion coefficient D_x profile.

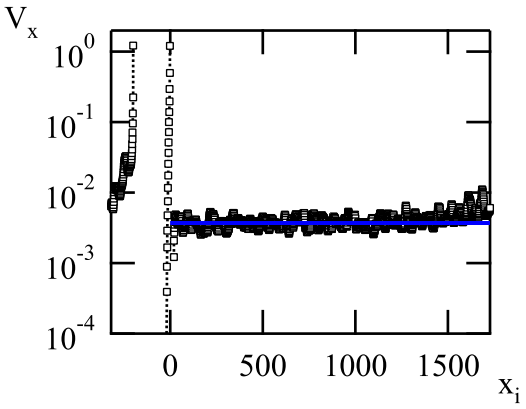

Figure 6. Velocity V_x profile.

4. Macroscopic transport analysis

Considering discretised transport operators, one can analyse the profile averaged in y and time either in terms of a profile of diffusive transport or in terms of a profile of convective transport, where the local diffusion D_x and convection V_x coefficients are defined according to the formulas:

$$D_x = \frac{\sigma_n n_i - S_i}{n_{i+1} + n_{i-1} - 2n_i} (\delta x)^2 \qquad ; \qquad V_x = \frac{2\left(\sigma_n n_i - S_i\right)}{n_{i+1} - n_{i-1}} \delta_x \tag{3}$$

Here the subscript i describes the discretised x-direction with a step δx. The result of the calculation is displayed on figure 5 and 6 clearly indicates that the values of the D_x exhibit a much larger fluctuation range than that of V_x. These fluctuations are clearly governed by the underlying turbulent transport since one properly recovers the value of $D = 10^{-2}$ in the stable region. Moreover, one finds that the values of D_x are reminiscent of a step like density profile with a sequence of small values followed by a large value. Based on these statistical properties, one would tend to consider that transport is more properly represented by a convection $< V_x >$ rather than the diffusion $< D_x >$ following therefore the microscopic properties. The macroscopic particle flux would then be of the form $< \Gamma_x > = < V_x > n$. However, from a thermodynamical point of view, the only force in the system is the density radial variation, hence the non-vanishing value of $-\nabla_x n$. Since the particle flux must be driven and opposite to the thermodynamical force, one expects recovering at lowest order a Fick law of the form $< \Gamma_x > = -\mathcal{D} \nabla_x n$. The mean density profile analysis does not appear to provide sufficient insight into the transport properties. One reason, already addressed in Section 2 could be the slow convergence of the

statistics due to the occurrence of large and rare transport events that generate the departure from an exponential solution with a step like structure. In order to overcome this difficulty, and

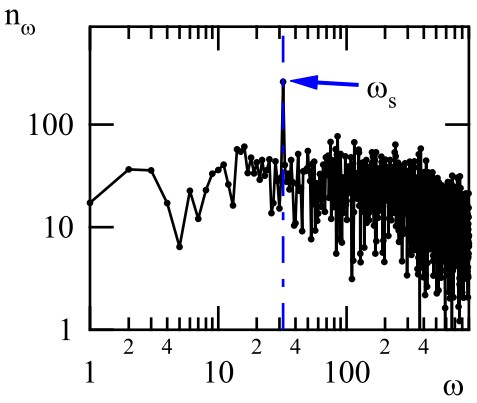

Figure 7. ω-spectrum of the density for a point in region I.

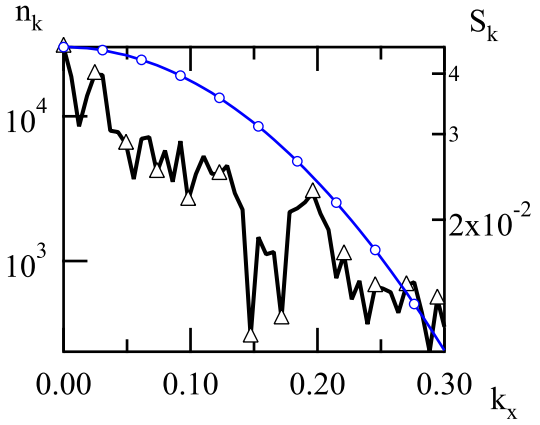

Figure 8. Source (open circles) and density (open triangles) k-spectra.

to investigate the possible coexistence of diffusion and convection, we have performed a series of simulations with a source modulation. The modulated source is localised in the same region as the main source, it is also constant along the y-direction and narrower in the x-direction, yielding a broad k_x spectrum. With the chosen value of the magnitude of the modulated source one identifies very well the density response at the source frequency ω_s, figure 7. One can then consider the transport equation in Fourier space:

$$\sigma_n - i\omega_s + \left(\mathrm{D_{eff}} k_x^2 + i \mathrm{V_{eff}} k_x\right) \quad = \quad \frac{\hat{S}}{\hat{n}} \tag{4}$$

where we have assumed the macroscopic, or effective, transport to be of the standard form $\Gamma = -\mathrm{D_{eff}} \nabla_x n + \mathrm{V_{eff}}\ n$. In such a framework the real part of the ratio $\hat{S}/\hat{n}$ should be a quadratic function of k_x while the imaginary part should be linear. The frequency ω_s must be small enough to allow the transport wave to propagate from the source to a sufficiently large distance, but not that large that it only drives an adiabatic response of the system at quasi-constant profile but slowly varying particle content. A value comparable to σ_n thus appears to be optimum. At any rate, as exemplified on figure 7, it is not possible to find a frequency outside the broad range of the turbulence spectrum. As expected for a system characterised by heavy tails of large transport events, there is no obvious time separation between turbulence and transport. No correlation between the source and density k_x-spectra has been observed, see figure 8. In particular, a signature of diffusive transport would govern a quadratic shape of the density spectrum at $k_x \to 0$ that must be more pronounced than that of the source, which is clearly not the case on figure 8 where the density spectrum is exponential like.

The two first transport analysis are based on a coarse graining process achieved by flux surface averaging, maximum coarse graining in y, and either averaging in time or selecting small frequencies both governing strong coarse graining in t.

We now analyse the impact of the coarse graining process by considering directly the particle flux $\langle \Gamma \rangle_{cg}$. The minimum coarse graining that is considered is a y-average to ensure that most of the data is consistent with the thermodynamical (macroscale) constraint of particle flux directed

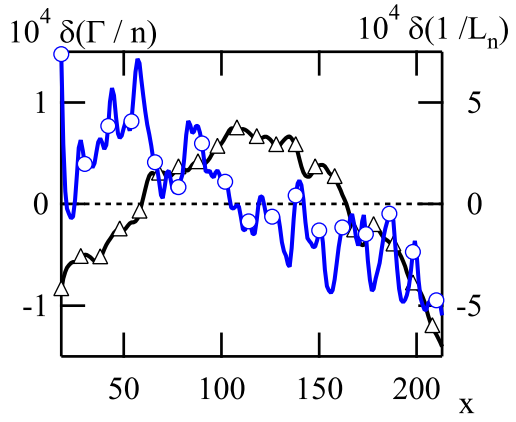

Figure 9. Blow up of the profiles of $\delta(\Gamma/n) = \Gamma/n - \langle\Gamma/n\rangle_x$, open triangles, and $\delta(1/L_n) = 1/L_n - \langle 1/L_n\rangle_x$, open circles.

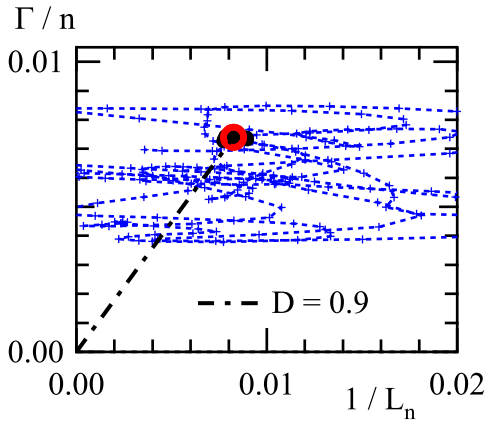

Figure 10. Γ/n as a function of $1/L_n$, y-average crosses and dashed lines, y and t average closed circles, x, y and t average open circle.

from the source towards the sink. One can expect $\langle\Gamma\rangle_{cg} / \langle n\rangle_{cg}$ to exhibit a polynomial expansion in $1/L_n$. In a linear expansion, consistent with weak departure from equilibrium the constant offset value would then be the convection velocity while the slope would be the diffusion coefficient. Data is selected from region I, figure 10, and does not appear to yield any trend, similarly to experimental evidence [9]. It is clear from this data that any relationship between $\langle\Gamma\rangle_{cg} / \langle n\rangle_{cg}$ and $1/L_n$ requires coarse graining in time. This is done by averaging over the duration of the simulation $t_s \approx 40\tau_E$. The data points exhibit more dispersion in $1/L_n$ than in $\langle\Gamma\rangle_{cg} / \langle n\rangle_{cg}$, figure 9. One then readily notices that the variation of $\langle\Gamma\rangle_{cg} / \langle n\rangle_{cg}$ is small and uncorrelated with the radial modulation of $1/L_n$. Again this data appears to be consistent with transport governed by convection. A response that is not possible since the system is governed by a single thermodynamical force measured by $1/L_n$. One is thus led to introduce coarse graining in x, here over region I to remove the profile effects, figure 9. The bottom line of this coarse graining process is that we have averaged over all possible direction to recover the Fick law, $\langle\Gamma_x\rangle_{cg} / \langle n\rangle_{cg} = -\mathcal{D}\langle 1/L_n\rangle_x$ represented by a single point on figure 10. In this process region I of the system is reduced to a single point, hence to a single reservoir interacting with other reservoirs. The single scalar characterising this reservoir, $\mathcal{D} \approx 0.9$, is equivalent to setting a characteristic evolution time $\tau = \mathcal{L}_x^2/\mathcal{D}$ where $\mathcal{L}_x \approx 190$ is the radial extent of region I, hence $\tau \approx 2.5\tau_E$. Some optimisation in the coarse graining process, different from the full time and radial coarse graining might be possible. Given the lack of correlation between the force and flux profiles in region I, figure 9, one can consider that the radial coarse graining cannot be modified while reducing the time coarse graining to τ might be possible.

5. Discussion and conclusion

We have shown in this paper that capturing the macroscale properties of a system driven by turbulence with self-organised transport events, avalanches or fronts, requires a strong coarse graining procedure. For the model we have implemented, this minimum coarse graining process includes a flux surface average (y-direction of the model), an average over the whole radial region and at least over times that correspond to a couple of confinement times. As a consequence, the total system appears to be reduced to only a few interacting reservoirs, the size of the latter being constrained by the requirement to have sufficient internal statistics to define an equilibrium

thermodynamical state, these define therefore macroscale regions. With the available simulation run time, the evolution of such a reservoir is limited to a few steps. With such a level of coarse graining the Fick law is recovered, but the information regarding the reservoir is reduced to a single scalar, akin to a confinement time. The consequence would thus be that in the present system, the existence of the Fick law does not imply diffusive transport at the microscale. At the macroscale, where diffusion appears to be legitimate, the few interacting reservoirs makes a discussion of transport in terms of diffusion rather artificial since only a couple of steps separate the boundary conditions.

This result can be understood in the framework of avalanche like transport events. These events are localised in space but rather long lived in time, hence leading to a long range transport structure. They appear to propagate with a ballistic motion, with nearly constant velocity magnitude but varying direction in the plane orthogonal to the magnetic field. The order of magnitude of the poloidal component being comparable to that of the radial component. The heavy tail structure of transport events they encompass drives a very slow convergence of the statistics. The duration of the random events τ_N that governs this process appears to be large, so that only several such events occur during a confinement time. Present investigation of the time lag between the avalanches appears to be consistent with τ_N of the order of the shortest time lag of the events belonging to the heavy tail structure of the particle flux. These transport processes that are a key signature of global and flux driven systems cannot be captured by approaches that introduce scale separation, e.g. *à la quasilinear*. This is very clear in particular when considering a scale separation between a given gradient scale (assumed to be a macroscale quantity) and the underlying scale of the fluctuations. Indeed the avalanche events lead to fast transport over significant fractions of the radial extent of the domain, while remaining localised. This is shown to lead to broad spectra (partly as a consequence of the localisation) such that scale separation in time or in space cannot be justified.

Avalanche like events are also reported in global flux driven gyrokinetic simulations of the core plasma with ITG turbulence. In these systems the sink is not volumetric as in the present model but localised at the boundary layer. Although the latter point can modify some aspects of the present description, one can expect that the avalanche transport in gyrokinetics will also hinder scale separation and consequently require strong coarse graining to recover macroscale thermodynamical properties. This is the matter of our present effort in analysing gyrokinetic simulations performed with the GYSELA code.

Acknowledgments

This work was supported by ANR grants ESPOIR ANR-09-BLAN-0035-01 and GYPSY ANR-10-BLAN-941, as well as the European Community under the contract of Association between EURATOM, CEA, and the French Research Federation for fusion study. The views and opinions expressed herein do not necessarily reflect those of the European Commission.

References

[1] N G Van Kampen 1981 *Stochastic Processes in Physics and Chemistry* (Amsterdam: North Holland)
[2] Y Sarazin *et al.* 2010 *Nucl. Fusion* **50** 054004
[3] S Jolliet and Y Idomura 2012 *Nucl. Fusion* **52** 023026
[4] G Dif-Pradalier, P H Diamond, V Grandgirard, Y Sarazin, J Abiteboul *et al.* 2010 *Phys. Rev. E* **82** 025401(R)
[5] Y Sarazin, V Grandgirard, J Abiteboul, S Allfrey, X Garbet *et al.* 2011 *Nucl. Fusion* **51** 103023
[6] Y Sarazin and Ph Ghendrih 1998 *Physics of Plasmas* **5** 4214
[7] S I Krasheninnikov 2001 *Physics Letters* A **283** 368
[8] Ph Ghendrih , Y Sarazin, G Attuel *et al.* 2005 *J. Nucl. Mater.* **337-339** 347
[9] O E Garcia, R A Pitts, J Horacek, A H Nielsen, W. Fundamenski *et al.* 2007 *J. Nucl. Mater.* **363-365** 575